2016 American Control Conference (ACC)
Boston Marriott Copley Place
July 6-8, 2016. Boston, MA, USA

Prosthetic Leg Control in the Nullspace of Human Interaction

Robert D. Gregg, *Member, IEEE* and Anne E. Martin

***Abstract*— Recent work has extended the control method of virtual constraints, originally developed for autonomous walking robots, to powered prosthetic legs for lower-limb amputees. Virtual constraints define desired joint patterns as functions of a mechanical phasing variable, which are typically enforced by torque control laws that linearize the output dynamics associated with the virtual constraints. However, the output dynamics of a powered prosthetic leg generally depend on the human interaction forces, which must be measured and canceled by the feedback linearizing control law. This feedback requires expensive multi-axis load cells, and actively canceling the interaction forces may minimize the human's influence over the prosthesis. To address these limitations, this paper proposes a method for projecting virtual constraints into the nullspace of the human interaction terms in the output dynamics. The projected virtual constraints naturally render the output dynamics invariant with respect to the human interaction forces, which instead enter into the internal dynamics of the partially linearized prosthetic system. This method is illustrated with simulations of a transfemoral amputee model walking with a powered knee-ankle prosthesis that is controlled via virtual constraints with and without the proposed projection.**

I. Introduction

A quintessential challenge in human-machine interaction is controlling a powered prosthetic leg to cooperate with its human user. A prosthetic leg and its user interact through forces at the socket, which is the intersection of the human's residual limb and the prosthesis. Through these interaction forces the human is able to influence the dynamics of the prosthesis and vice versa. These forces thus determine the level of cooperation between human and machine, which must be considered when designing a prosthesis controller.

Previous control system designs for powered prosthetic legs have dealt with human interaction in different ways. In the traditional paradigm of impedance control [1]–[3], stiffness and viscosity gains for different phases of the gait cycle are tuned with implicit consideration of the interaction forces typically encountered in those phases, e.g., load acceptance during early stance. A more recent approach explicitly considers the interaction forces when designing controllers that are robust to them under normal circumstances [4], [5]. Although these two approaches have the practical benefit of not requiring interaction force measurements for feedback control, they are unable to accommodate unexpected interactions associated with changes in the human user's behavior.

A third approach, based on input-output feedback linearization [6], directly measures the human interaction forces in real time to actively cancel their influence on control objectives [7], [8]. In this paradigm the control objective is to enforce virtual constraints, which define desired joint trajectories as functions of a mechanical phasing variable. The desired constraints are enforced by torque control laws that linearize and stabilize the input-output dynamics associated with the constraint outputs. This method has been widely successful in controlling autonomous walking robots without human interaction [9]–[17]. In the application to powered prosthetic legs, the input-output dynamics generally depend on the human interaction forces, through which the human can influence the behavior of the leg. For example, the human could force desired changes in the prosthetic joint kinematics as the task or environment changes. However, linearizing the prosthesis input-output dynamics through active cancelation of the human interaction forces would ensure that the prosthesis tracks the fixed reference trajectories regardless of the human's intent. This strategy would also require expensive multi-axis load cells to measure the interaction forces.

To address these limitations with feedback linearizing control of prosthetic legs, this paper proposes a method for projecting virtual constraints into the nullspace of the human interaction terms in the input-output dynamics. The projected virtual constraints naturally render the input-output dynamics invariant with respect to the human interaction forces, which instead enter into the internal dynamics of the partially linearized prosthetic system. We prove controllability of the projected input-output dynamics during the prosthesis swing period and demonstrate controllability for a partial projection during the prosthesis stance period. This method is illustrated with simulations of a transfemoral amputee model walking with a powered knee-ankle prosthesis that is controlled via virtual constraints with and without the proposed projection. These simulations support the hypothesis that projected virtual constraints could provide lower-limb amputees with more control over (or less resistance from) their prosthesis.

II. Prosthetic Virtual Constraints

This paper considers the case of a unilateral above-knee amputee walking with a powered knee-ankle prosthesis. The prosthetic leg depicted in Fig. 1 is rigidly attached to the residual thigh (i.e., stump) of the "human" body, so these two parts can be modeled as separate dynamical systems that are coupled through interaction forces. The kinematic chains for

Asterisk indicates corresponding author.
R.D. Gregg* is with the Departments of Bioengineering and Mechanical Engineering, University of Texas at Dallas, Richardson, TX 75080, USA. rgregg@ieee.org
A.E. Martin is with the Department of Mechanical and Nuclear Engineering, Pennsylvania State University, State College, PA 16801, USA.
This work was supported by the National Institute of Child Health & Human Development of the NIH under Award Number DP2HD080349. The content is solely the responsibility of the authors and does not necessarily represent the official views of the NIH. R. D. Gregg holds a Career Award at the Scientific Interface from the Burroughs Welcome Fund.

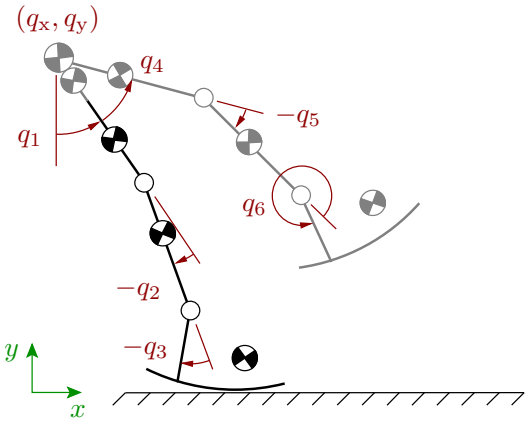

Fig. 1. Schematic of the unilateral, transfemoral amputee model during the prosthesis stance period (reproduced from [8]). The prosthetic part is shown in black and the human part is shown in gray. The q terms define the generalized coordinates of the model. Absolute angle q_1 is unactuated and relative angles q_2-q_6 have ideal actuators. Dorsiflexion/plantarflexion of the stance ankle and extension/flexion of the stance knee are defined in the positive/negative directions.

both parts are defined with respect to the same inertial reference frame on the ground (Fig. 1). Because the prosthesis is rigidly attached to the human's residual thigh, the prosthesis and human models can share the same global coordinates defined at the residual thigh. The generalized coordinates of both parts begin with the Cartesian coordinates (q_x, q_y) of the hip and the absolute angle q_1 of the residual thigh. The rest of this section focuses on the modeling and control of the prosthesis, but the human part will be considered for the purpose of simulation in Section IV.

A. Modeling a Powered Knee-Ankle Prosthesis

The dynamical system of the prosthetic leg is modeled as in [7], [8]. The configuration of the prosthesis in configuration space $\mathcal{Q} = \mathbb{R}^2 \times \mathbb{T}^3$ is given by $q = [q_x, q_y, q_1, q_2, q_3]^T$, where q_1 is the absolute thigh angle, q_2 is the knee angle, and q_3 is the ankle angle. The system state is then given by the vector $x = [q^T, \dot{q}^T]^T \in T\mathcal{Q}$, where $\dot{q} \in \mathbb{R}^5$ contains the joint velocities. The state trajectory evolves according to a differential equation of the form

$$M(q)\ddot{q} + C(q,\dot{q})\dot{q} + G(q) + A(q)^T\lambda = Bu + J(q)^T F \quad (1)$$

where $M \in \mathbb{R}^{5\times5}$ is the inertia/mass matrix, $C \in \mathbb{R}^{5\times5}$ is the matrix of Coriolis/centrifugal terms, $G \in \mathbb{R}^5$ is the vector of gravitational forces, $A \in \mathbb{R}^{c\times5}$ is the matrix modeling c physical constraints between the foot and ground, and $\lambda \in \mathbb{R}^c$ is the Lagrange multiplier used to calculate the contact forces. The external forces on the right-hand side of (1) respectively comprise actuator torques and interaction forces with the body. Ankle and knee actuation from torque input $u \in \mathbb{R}^2$ are mapped into the leg's coordinate system by $B = [0_{2\times3}, I_{2\times2}]^T \in \mathbb{R}^{5\times2}$. The interaction force $F = [F_x, F_y, M_z]^T \in \mathbb{R}^3$ at the socket—the connection between the prosthesis and body at the mid-thigh in Fig. 1—comprises two linear forces and a moment in the sagittal plane [7]. Force vector F acts at the beginning of the leg's kinematic chain and is mapped to joint torques/forces by the *body Jacobian* matrix $J(q) = [J_1, 0_{3\times2}] \in \mathbb{R}^{3\times5}$, where

$$J_1 = \begin{bmatrix} 1 & 0 & \ell_{\text{res}}\cos(q_1) \\ 0 & 1 & \ell_{\text{res}}\sin(q_1) \\ 0 & 0 & 1 \end{bmatrix} \quad (2)$$

and ℓ_{res} is the length of the human's residual thigh.

The presence of contact forces depends on whether the prosthetic leg is in stance or swing. The prosthetic part is in stance when the human part is in swing, and vice versa.

1) Swing Period: The prosthetic foot is not in contact with the ground during the prosthesis swing period, so no contact constraints are invoked in the prosthesis dynamics, i.e., $A = 0$ and $\lambda = 0$ in (1). The interaction force vector F in prosthesis dynamics (1) suspends the prosthetic leg from the human's residual thigh.

2) Stance Period: The physical forces associated with contact between the prosthetic foot and ground are modeled during the prosthesis stance period. These contact forces prevent the foot from slipping and falling through the ground, which constitute at least two physical constraints on dynamics (1). Therefore, foot geometry is commonly modeled (e.g., [7], [8], [14], [18], [19]) as a vector holonomic constraint

$$a(q) = 0, \quad (3)$$

where $a : \mathcal{Q} \to \mathbb{R}^c$ for $c \geq 2$. We will employ the rocker foot depicted in Fig. 1 for one continuous stance phase ($c = 2$), but other contact models such as heel, flat foot, and toe contact [19] could similarly be modeled in this framework.

Given the rolling contact constraint $a(q) = 0$ from [8], [14], [18], we follow the method in [7], [20] to compute the constraint matrix $A = \nabla_q a$ and the Lagrange multiplier

$$\begin{aligned} \lambda &= \widehat{\lambda} + \widetilde{\lambda}u + \bar{\lambda}F, \text{ where} \\ \widehat{\lambda} &= V(\dot{A}\dot{q} - AM^{-1}(C\dot{q} + G)), \\ \widetilde{\lambda} &= VAM^{-1}B, \quad \bar{\lambda} = VAM^{-1}J^T \end{aligned} \quad (4)$$

for $V = (AM^{-1}A^T)^{-1}$. These terms enter into dynamics (1) only during the stance period of the prosthetic leg.

B. Definition of a Virtual Constraint

Although defined in a similar manner to physical/contact constraints, virtual constraints are enforced by actuator torques rather than external physical forces. The vast majority of virtual constraints used in bipedal robots are holonomic [9]–[17], so we consider virtual holonomic constraints

$$h(q) = 0, \quad (5)$$

where $h : \mathcal{Q} \to \mathbb{R}^2$ for an actuated knee and ankle, i.e., one virtual constraint per actuated degree-of-freedom (DOF).

Virtual constraints, i.e., output functions $h(q)$, can be defined in a variety of ways. In previous work on bipedal robots (e.g., [9]–[17]), virtual constraints are used to control the actuated joints specified by $h_0(q) = (q_2, q_3)^T$ to a desired trajectory $h_d(\Theta(q)) \in \mathbb{T}^2$ as a function of a monotonic

quantity $\Theta(q) \in \mathbb{R}$. This quantity, known as the *phase variable* (or *timing variable*), provides a unique representation of the gait cycle phase to drive forward the desired joint patterns in a time-invariant manner. The output function on the left-hand side of constraint (5) is typically defined as $h(q) = h_0(q) - h_{\rm d}(\Theta(q))$, but we will introduce another definition via nullspace projection in Section III.

Given a desired virtual constraint (5) defined by an output function $h(q)$, the goal of the controller is to drive $h(q)$ to zero. Therefore, the control system output $y = h(q)$ is the tracking error from the desired constraint (5).

C. Normal Form of the Prosthesis Dynamics

The temporal behavior of any given output $y = h(q) \in \mathbb{R}^2$ can be determined from its input-output dynamics, hereafter referred to as the *output dynamics*. These dynamics are obtained by taking time-derivatives of y until the input u appears. The first derivative is trivially given by $\dot{y} = (\nabla_q h)\dot{q}$, implying the output y has relative degree greater than one (cf. [6]) and another time-derivative is needed. Letting $H = \nabla_q h$, the output dynamics are obtained by

$$\begin{aligned} \ddot{y} &= \dot{H}\dot{q} + H\ddot{q} \\ &= \dot{H}\dot{q} + HM^{-1}(-C\dot{q} - G - A^T\lambda + Bu + J^T F). \end{aligned}$$

Plugging in (4) for λ, we obtain the form

$$\begin{aligned} \ddot{y} &= \dot{H}\dot{q} - HM^{-1}(C\dot{q} + G + A^T\widehat{\lambda}) \\ &\quad + HM^{-1}B_\lambda u + HM^{-1}J_\lambda^T F, \end{aligned} \tag{6}$$

where we have adopted from [19] the notation

$$B_\lambda = (B - A^T\widetilde{\lambda}) = UB \tag{7}$$

$$J_\lambda = (J^T - A^T\bar{\lambda})^T = JU^T \tag{8}$$

with $U = I - A^T V A M^{-1}$. It is clear that B_λ and J_λ reduce to B and J, respectively, in the absence of ground contact.

These output dynamics account for 4 of the 10 dimensions of the system defined by (1). The remaining dimensions correspond to the *internal dynamics* of the input-output system. A decomposition of the output and internal dynamics can be obtained through a straight-forward generalization of a classical result in [21]. Given sufficiently smooth vector fields over a compact subset $D \subset T\mathcal{Q}$, for every state $x_0 \in D$ there exists a map $T(x) = (\eta^T, \xi^T)^T$ such that $T(x)$ is a local coordinate transformation of system (1) on a neighborhood of x_0 to the *normal form*

$$\dot{\eta} = f_0(\eta, \xi) + j_0(\eta, \xi)F \tag{9}$$

$$\dot{\xi} = \mathcal{A}_c\xi + \mathcal{B}_c\rho_0(\eta, \xi)\left(u - \alpha_0(\eta, \xi) - \beta_0(\eta, \xi)F\right), \tag{10}$$

where $\eta \in \mathbb{R}^6$ are the coordinates of the internal dynamics (9), and $\xi = [y^T,\ \dot{y}^T]^T \in \mathbb{R}^4$ are the coordinates of the normal output dynamics (10), which is the first-order representation of (6). These two coupled systems are defined by vector fields $f_0 \in \mathbb{R}^{6\times 1}$, $j_0 \in \mathbb{R}^{6\times 3}$, $\rho_0 \in \mathbb{R}^{2\times 2}$, $\alpha_0 \in \mathbb{R}^{2\times 1}$, and $\beta_0 \in \mathbb{R}^{2\times 3}$ and a matrix pair $(\mathcal{A}_c, \mathcal{B}_c)$, which is the canonical form representation of a 2-integrator chain (see [21] for details). It is important to note that the human interaction force F enters both subsystems, but the control input u only enters the output dynamics (10).

Recent work in prosthetics [7], [8] has utilized input-output feedback linearization to stabilize the output dynamics (10) and drive y to zero exponentially fast, but this approach has two key problems that we wish to address in this paper. These prior control strategies depend on real-time measurements of the interaction force vector F to cancel out its effect on the output dynamics, requiring expensive (and noisy) multi-axis force sensors. Given that the interaction forces are the human's control inputs to the prosthetic leg, the cancellation of these forces in (10) may also reduce the human's control authority over the prosthesis. The human would not be able to force adjustments in the prosthesis kinematics to accommodate changes in task or environment.

The goal of the next section—the main contribution of the paper—is to render the open-loop output dynamics (6) and (10) invariant with respect to the human interaction forces through the design of the output matrix H. By making the output dynamics invariant, the interaction forces will only enter the internal dynamics (9) of the prosthesis, which are untouched by the input-output linearization. We speculate that the human will have more control over (or less resistance from) the prosthesis when their interaction forces are not actively canceled in either subsystem (9)–(10).

III. Projection of Virtual Constraints

In this section a desired/reference virtual constraint will be projected into the human interaction nullspace to define a new virtual constraint that will ultimately be enforced by feedback control. Assume that the reference virtual constraint has been previously defined with a reference output $y_{\rm ref} = h_{\rm ref}(q)$ and its gradient $H_{\rm ref} = \nabla_q h_{\rm ref}$. Without loss of generality we will consider the form

$$h_{\rm ref}(q) = h_0(q) - h_{\rm d}(\Theta(q)) \tag{11}$$

as discussed in Section II-B. This reference output will be used to define the regulated/enforced output $y = h(q)$ associated with the output dynamics (6), but $h(q)$ will not have the same form as (11).

A. Swing Period

During the swing period the dynamics simplify with $\lambda = 0$, $B_\lambda = B$, and $J_\lambda = J$. To prevent the interaction forces from appearing in the open-loop output dynamics (6), we wish to convert $h_{\rm ref}(q) \in \mathbb{R}^2$ into $h(q) \in \mathbb{R}^2$ such that $H^T = (\nabla_q h)^T \in \mathcal{N}(JM^{-1})$, where $\mathcal{N}(\cdot)$ is the nullspace [22], i.e., $JM^{-1}H^T = 0_{3\times 2}$. We will follow the intuition behind hierarchical operational space control [23]–[25] to achieve a secondary task (enforcing the reference virtual constraint) to the extent possible while complying with the primary task (constrained to the human interaction nullspace).

Letting $J_{\rm c} = JM^{-1} \in \mathbb{R}^{3\times 5}$, the *nullspace projector*

$$N = I - J_{\rm c}^- J_{\rm c} \tag{12}$$

is defined with the generalized pseudo-inverse

$$J_{\rm c}^- = W J_{\rm c}^T (J_{\rm c} W J_{\rm c}^T)^{-1} \tag{13}$$

and a full-rank weight matrix W. It can be verified that the nullspace projector N has the property $J_c N H_{ref}^T = 0$ for any H_{ref}. Therefore the nullspace projector N maps a reference output matrix H_{ref}, corresponding to a desired virtual constraint $h_{ref}(q) = 0$, into the human interaction nullspace. The output matrix that enforces the desired constraint to the extent possible in the interaction nullspace is given by

$$H^T = N H_{ref}^T. \quad (14)$$

Choosing $W = M$ results in the following simplifications:

$$J_c^- = J^T (J M^{-1} J^T)^{-1} \quad (15)$$
$$N = I - J^T (J M^{-1} J^T)^{-1} J M^{-1}. \quad (16)$$

We can further simplify the nullspace projector based on the interaction Jacobian (2) of a knee-ankle prosthesis. Defining $\bar{M} = \begin{bmatrix} \bar{M}_1 & \bar{M}_2 \\ \bar{M}_2^T & \bar{M}_3 \end{bmatrix} = M^{-1}$ for notational convenience, the nullspace projector becomes

$$N = \begin{bmatrix} 0 & -\bar{M}_1^{-1}\bar{M}_2 \\ 0 & I \end{bmatrix}. \quad (17)$$

Letting $M_1 \in \mathbb{R}^{3\times3}$, $M_2 \in \mathbb{R}^{3\times2}$, and $M_3 \in \mathbb{R}^{2\times2}$ be the top-left, top-right, and bottom-right submatrices of M, respectively, a blockwise inverse [26] gives

$$\bar{M}_1 = (M_1 - M_2 M_3^{-1} M_2^T)^{-1}$$
$$\bar{M}_2 = -(M_1 - M_2 M_3^{-1} M_2^T)^{-1} M_2 M_3^{-1},$$

Noting that $\bar{M}_1^{-1}\bar{M}_2 = -M_2 M_3^{-1}$, the projected output matrix simplifies to

$$H^T = \begin{bmatrix} -\bar{M}_1^{-1}\bar{M}_2 H_{ref2}^T \\ H_{ref2}^T \end{bmatrix} = \begin{bmatrix} M_2 M_3^{-1} H_{ref2}^T \\ H_{ref2}^T \end{bmatrix}, \quad (18)$$

where H_{ref2}^T is the lower 2×2 submatrix of H_{ref}^T. These simplifications to the projection (12) resulted in the inversion of a 2×2 matrix instead of the entire M matrix. Thus the projected virtual constraints should not significantly increase computational costs or sensitivity to modeling errors [23].

The new output $y = h(q)$ must be chosen such that $\nabla_q h$ is equal to the $H(q)$ derived in (18), but the function $h(q)$ can be difficult to obtain analytically. Given that $\dot{y} = H\dot{q}$ is easily determined, the output trajectory can be calculated as $y(t) = y(0) + \int_0^t H(q(\tau))\dot{q}(\tau)d\tau$. The initial condition can be chosen as $y(0) = y_{ref}(0)$, where $y_{ref}(q)$ is known. However, we will later avoid this step by trying to zero the original output $y_{ref}(t)$ in the projected output dynamics.

B. Stance Period

When $A \neq 0$ in the open-loop output dynamics (6), we must design $h(q)$ such that $H^T = (\nabla_q h)^T \in \mathcal{N}(J_\lambda M^{-1})$, i.e., $J_\lambda M^{-1} H^T = 0_{3\times2}$. Let $J_{c\lambda} = J_\lambda M^{-1}$ and $W = (U^T M^{-1})^{-1}$. Noting that $J_{c\lambda} = JW^{-1}$, the generalized pseudo-inverse takes the form

$$J_{c\lambda}^- = W J_{c\lambda}^T (J_{c\lambda} W J_{c\lambda}^T)^{-1} = J^T (J W^{-1} J^T)^{-1}. \quad (19)$$

Then we obtain the nullspace projector following the same procedure as before:

$$N_\lambda = I - J^T (J W^{-1} J^T)^{-1} J W^{-1}. \quad (20)$$

For the prosthesis model the projector simplifies to

$$N_\lambda = \begin{bmatrix} 0 & W_2 W_3^{-1} \\ 0 & I \end{bmatrix}, \quad (21)$$

so the projected output matrix becomes

$$H^T = N_\lambda H_{ref}^T = \begin{bmatrix} W_2 W_3^{-1} H_{ref2}^T \\ H_{ref2}^T \end{bmatrix}. \quad (22)$$

The output function $y = h(q)$ can then be defined as in the contact-free case. It is clear that (22) reduces to (18) in the absence of ground contact because U becomes identity.

This choice of output function results in the projected second-order output dynamics

$$\ddot{y} = \dot{H}\dot{q} - H M^{-1}(C\dot{q} + G + A^T \widehat{\lambda}) + H M^{-1} B_\lambda u, \quad (23)$$

which are invariant with respect to the interaction force vector. The projected output dynamics of the swing period have the same form with $B_\lambda = B$ and $\widehat{\lambda} = 0$.

A variety of control methods (e.g., proportional-derivative control [27], finite-time control [9], acceleration-based inverse dynamics [25], control Lyapunov functions [28], [29], and/or input-output feedback linearization [7]) can be employed to drive output y to zero. In all cases the interaction forces have no effect on the transient or steady-state behavior of the closed-loop output dynamics after the projection.

C. Controllability of Projected Output Dynamics

We wish to project the virtual constraints into the human interaction nullspace without losing control in the projected output dynamics (23). If any column of H^T is in $\mathcal{N}(B_\lambda^T M^{-1})$, then the decoupling matrix

$$D_\lambda = H M^{-1} B_\lambda \quad (24)$$

is singular, and some (or all) control authority is lost in (23). This situation is avoided if H^T lies in an orthogonal vector space to $\mathcal{N}(B_\lambda^T M^{-1})$, which is the range space $\mathcal{R}(M^{-1}B_\lambda)$ [22]. Therefore, the goal is to ensure

$$H^T \in \mathcal{R}(M^{-1}B_\lambda) \cap \mathcal{N}(J_\lambda M^{-1}). \quad (25)$$

Theorem 1: During the swing period ($A = 0$), condition (25) is guaranteed by H defined as (18). I.e., the prosthesis output dynamics (6) are controllable by actuator torques and invariant with respect to the human interaction forces.

Proof: By inspection of model terms in Section II-A, $B \in \mathbb{R}^{5\times2}$ and $J^T \in \mathbb{R}^{5\times3}$ lie in orthogonal vector spaces, i.e., $JB = 0_{3\times2}$. This implies that $\mathcal{R}(M^{-1}B) = \mathcal{N}(JM^{-1})$ given the invertibility of M^{-1}. Because (18) satisfies $H^T \in \mathcal{N}(J_\lambda M^{-1})$, condition (25) is equivalently satisfied. ■

However, the stance period is not so obvious. From (7)–(8) we can see that J_λ^T and B_λ may not lie in orthogonal vector spaces. In fact, it may be possible that $\mathcal{R}(M^{-1}B_\lambda) \cap \mathcal{N}(J_\lambda M^{-1})$ is an empty set during stance. In

other words, the decoupling matrix D_λ may become singular in the presence of nullspace constraints (3 dimensions) *and* contact constraints (2 dimensions) for the 5-dimensional configuration space. Removing the nullspace constraint(s) corresponding to certain interaction force direction(s) may restore controllability to the output dynamics.

Let matrix $S \in \mathbb{R}^{k\times 3}$, $1 \leq k \leq 3$, be a *selector* matrix[1] that selects the interaction force directions that will define the nullspace projection. (Previously all three force directions were utilized, corresponding to $S = I$.) The new nullspace projection is defined by (20) with $J_S = SJ$ so that the selected directions in F vanish in the output dynamics (6). Noting that $\mathcal{N}(J_\lambda M^{-1}) \subset \mathcal{N}(SJ_\lambda M^{-1})$, the design of H in (22) must now satisfy the relaxed condition

$$H^T \quad \in \quad \mathcal{R}(M^{-1}B_\lambda) \cap \mathcal{N}(SJ_\lambda M^{-1}). \tag{26}$$

Because virtual constraints must be linearly independent [9], the dimension of the intersection set in (26) must be at least 2, the rank of H. The dimension of this set depends on the choice of S, which will be discussed in the following section.

IV. Application to Amputee Locomotion

For demonstration purposes we utilize the knee-ankle virtual constraints in [8] as the reference output function $h_{\mathrm{ref}}(q) = h_0(q) - h_{\mathrm{d}}(\Theta(q)) \in \mathbb{R}^2$ that defines H_{ref}, where different output functions are used for the stance and swing periods of the prosthesis. These outputs were manually chosen to approximate the joint kinematics of healthy human gait and were parameterized using fifth-order Bézier polynomials [8]:

$$h_d(\Theta(q)) = \sum_{i=0}^{5} \frac{a_i 5!}{i!(5-i)!} s^i (1-s)^{5-i}, \tag{27}$$

where $s = (\Theta - \Theta^+) / (\Theta^- - \Theta^+)$ is the normalized phase variable such that $0 \leq s \leq 1$, a_i are the polynomial coefficients, the superscript '$-$' indicates the end of a stance period, and the superscript '$+$' indicates the start of a stance period. The horizontal hip position was chosen as the phase variable, i.e., $\Theta(q) = q_{\mathrm{x}}$, but other options exist [30].

A. Input-Output Linearizing Control Law

Our goal is to define a feedback control law for input u that drives output y to zero in the projected output dynamics (23). Input-output feedback linearization [6] can be utilized for this purpose. If the 2×2 decoupling matrix D_λ is invertible over feasible walking configurations, we can solve for the control law that inverts the projected output dynamics (23):

$$u_{\mathrm{linz}} = D_\lambda^{-1}(-\dot{H}\dot{q} + HM^{-1}(C\dot{q} + G + A^T\widehat{\lambda}) + v_{\mathrm{pd}}), \tag{28}$$

which does not depend on the interaction force vector F.

The projected output dynamics then become the double-integrator $\ddot{y} = v_{\mathrm{pd}}$, which can be stabilized with a linear input v_{pd}. This input is typically chosen as proportional-derivative (PD) corrections of y to exponentially drive it to zero [7]. In our case, better tracking of the reference joint trajectories might be achieved using PD corrections of the reference output y_{ref}:

$$\begin{aligned} v_{\mathrm{pd}} &= -K_{\mathrm{p}} y_{\mathrm{ref}} - K_{\mathrm{d}} \dot{y}_{\mathrm{ref}} \\ &= -K_{\mathrm{p}} h_{\mathrm{ref}}(q) - K_{\mathrm{d}} H_{\mathrm{ref}}(q)\dot{q} \end{aligned} \tag{29}$$

with positive-definite $K_{\mathrm{p}}, K_{\mathrm{d}} \in \mathbb{R}^{2\times 2}$. The interaction forces only appear in the second derivative of y_{ref}, so interaction invariance is maintained when setting the projected acceleration $\ddot{y}$ equal to (29) for the closed-loop output dynamics

$$\ddot{y} \quad = \quad -K_{\mathrm{p}} y_{\mathrm{ref}} - K_{\mathrm{d}} \dot{y}_{\mathrm{ref}}. \tag{30}$$

Because the acceleration on the left-hand side of (30) does not exactly correspond to the position and velocity on the right-hand side, exponential stability cannot be guaranteed. However, if y and y_{ref} are sufficiently close and the PD gains are sufficiently large, reasonable (but not perfect) tracking of y_{ref} about zero can be achieved. This claim will be demonstrated in the simulations of Section IV-C.

In summary, exact enforcement of the reference virtual constraints has been sacrificed in order to avoid active cancelation of the human interaction forces. Only experiments with human subjects can tell whether this strategy is preferred over stricter enforcement of virtual constraints, but the simulations of Section IV-C will show that the inexact approach is at least sufficient for maintaining a stable walking gait.

1) Swing Control: The reference swing output matrix $H_{\mathrm{swref}} = \nabla_q h_{\mathrm{swref}}$ is obtained from [8]. According to Theorem 1, the decoupling matrix D_λ in (24) is invertible with H_{sw} obtained from the nullspace projection (18) of H_{swref} in all interaction force directions ($S = I$). Therefore the swing control law u_{sw} is given by (28).

2) Stance Control: Given the rolling contact constraint matrix A and the stance output matrix $H_{\mathrm{stref}} = \nabla_q h_{\mathrm{stref}}$ from [8], numerical analysis suggests that D_λ is invertible when projecting into the nullspace of the F_{x} direction, i.e., $S_{\mathrm{x}} = [1 \quad 0 \quad 0]$. Thus we define $H_{\mathrm{st}} = H_{\mathrm{stref}} N_\lambda^T$ with $J_{\mathrm{x}} = S_{\mathrm{x}} J$ in (20), resulting in a modified control law for the prosthesis stance period:

$$\begin{aligned} u_{\mathrm{st}} \quad = \quad & D_\lambda^{-1}(-\dot{H}_{\mathrm{st}}\dot{q} + H_{\mathrm{st}} M^{-1}(C\dot{q} + G + A^T\widehat{\lambda}) \\ & - H_{\mathrm{st}} M^{-1} J_{\lambda\mathrm{yz}}^T [F_{\mathrm{y}}, M_{\mathrm{z}}]^T + v_{\mathrm{pd}}), \end{aligned} \tag{31}$$

where $J_{\lambda\mathrm{yz}} = [0_{2\times 1} \quad I_{2\times 2}] J_\lambda$. This modified control law requires a two-axis load cell to measure the vertical force and the moment, i.e., no measurement of the horizontal force. Because the horizontal force is approximately in the direction of locomotion, the human user may have more control over walking speed when this force direction is not actively canceled by the prosthesis controller.

B. Modeling an Amputee Biped

In this section we model the complete amputee biped in Fig. 1 in order to simulate a prosthetic leg under control law (28). These simulations require us to consider the coupled dynamics of the human body and the prosthesis for a total of 8 DOFs. The extended configuration vector is denoted by $q_{\mathrm{e}} = [q^T, q_4, q_5, q_6]^T \in \mathcal{Q} \times \mathbb{T}^3$, where q is the prosthesis

[1]Each row of S can have only a single non-zero entry, equal to one.

configuration vector, q_4 is the body's hip (inter-leg) angle, q_5 is the body's knee angle, and q_6 is the body's ankle angle. The human and prosthetic feet are modeled as arcs with constant curvature as in [8], [14], [18]. After imposing the rolling contact constraints on the stance leg, the full biped has one degree of underactuation, the absolute angle q_1.

The human musculoskeletal control is modeled using input-output feedback linearization [18]. The human state dynamics modeled in [8] correspond to an equation with the same form as (1). Because the human virtual constraints do not lie in the prosthesis nullspace, the control law is

$$\begin{aligned} u_{\mathrm{H}} &= D_\lambda^{-1}(-\dot{H}_{\mathrm{H}}\dot{q}_{\mathrm{H}} + H_{\mathrm{H}}M^{-1}(C\dot{q}_{\mathrm{H}} + G + A^T\widehat{\lambda}) \\ &\quad -H_{\mathrm{H}}M^{-1}J_\lambda^T F + v_{\mathrm{pd}}), \end{aligned} \tag{32}$$

where the terms are the same as in (1) except defined for the human [8]. Similar to the prosthesis, the virtual constraints are defined separately for human stance and swing and are parameterized using fifth-order Bézier polynomials. Define $\tau_e \in \mathbb{R}^5$ as the concatenation of the prosthesis controller (given by (31) for the prosthesis stance period and (28) for the prosthesis swing period) and the human controller (32).

Bipedal locomotion involves both continuous and discrete dynamics, which constitute a hybrid dynamical system. The biped's continuous dynamics are governed by a differential equation of the form (1) with generalized coordinate vector q_{e}. One gait cycle comprises a sequence of the prosthetic stance period (continuous), human heel-strike (discrete with impact map Δ_{H}), the human stance period (continuous), and prosthetic heel-strike (discrete with impact map Δ_{P}):

$$\begin{aligned} M_{\mathrm{e}}\ddot{q}_{\mathrm{e}} + C_{\mathrm{e}}\dot{q}_{\mathrm{e}} + G_{\mathrm{e}} + A_{\mathrm{P}}^T\lambda_{\mathrm{P}} &= B_{\mathrm{e}}\tau_{\mathrm{e}}, \quad \text{if} \quad p_{\mathrm{H}}(q_{\mathrm{e}}) > 0 \\ (q_{\mathrm{e}}^+, \dot{q}_{\mathrm{e}}{}^+) &= \Delta_{\mathrm{H}}(q_{\mathrm{e}}^-, \dot{q}_{\mathrm{e}}{}^-), \quad \text{if} \quad p_{\mathrm{H}}(q_{\mathrm{e}}) = 0 \\ M_{\mathrm{e}}\ddot{q}_{\mathrm{e}} + C_{\mathrm{e}}\dot{q}_{\mathrm{e}} + G_{\mathrm{e}} + A_{\mathrm{H}}^T\lambda_{\mathrm{H}} &= B_{\mathrm{e}}\tau_{\mathrm{e}}, \quad \text{if} \quad p_{\mathrm{P}}(q_{\mathrm{e}}) > 0 \\ (q_{\mathrm{e}}^+, \dot{q}_{\mathrm{e}}{}^+) &= \Delta_{\mathrm{P}}(q_{\mathrm{e}}^-, \dot{q}_{\mathrm{e}}{}^-), \quad \text{if} \quad p_{\mathrm{P}}(q_{\mathrm{e}}) = 0 \end{aligned}$$

which then returns to the beginning of the sequence for the next step [7]. The dynamics account for the leg in contact with the ground by utilizing a constraint matrix A_i and GRF vector λ_i specific to the prosthetic leg ($i = \mathrm{P}$) or human leg ($i = \mathrm{H}$), which are modeled as in [8], [14], [18]. The function $p_i(q_{\mathrm{e}}) \in \mathbb{R}$ gives the height of the human or prosthetic swing heel, and the superscripts $+/-$ respectively denote post/pre-impact. Other extended dynamics terms are defined as in Section II-A with respect to the coordinate vector q_{e}.

The stability of a hybrid dynamical system can be analyzed with the method of Poincaré sections [9], [31]. Letting $x_{\mathrm{e}} = [q_{\mathrm{e}}^T, \dot{q}_{\mathrm{e}}{}^T]^T$ be the state vector of the full biped, walking gaits are cyclic and correspond to solution curves $x_{\mathrm{e}}(t)$ of the hybrid system such that $x_{\mathrm{e}}(t) = x_{\mathrm{e}}(t+T)$, for all $t \geq 0$ and some minimal $T > 0$. These solutions, known as *hybrid periodic orbits*, correspond to equilibria of the Poincaré map $P : G_{\mathrm{P}} \to G_{\mathrm{P}}$, where the Poincaré section $G_{\mathrm{P}} = \{x_{\mathrm{e}} | p_{\mathrm{P}}(q_{\mathrm{e}}) = 0\}$ corresponds to prosthesis heel strike. The function $P(x_{\mathrm{e}})$ models two full steps of the biped, mapping the state from a prosthesis heel strike event to the subsequent prosthesis heel strike event. A periodic solution $x_{\mathrm{e}}(t)$ then has a fixed point $x_{\mathrm{e}}^* = P(x_{\mathrm{e}}^*)$, about which the Poincaré map can be linearized to analyze local stability. If the eigenvalues are within the unit circle, then the discrete system is locally stable, and we conclude that the hybrid periodic orbit is also locally stable.

TABLE I
ORIGINAL VS. PROJECTED GAIT FEATURES

Original Gait	Prosthesis Stance	Prosthesis Swing
Step Length [m]	0.719	0.723
Step Duration [s]	0.448	0.434
Step Speed [m/s]	1.604	1.666
Projected Gait	Prosthesis Stance	Prosthesis Swing
Step Length [m]	0.696	0.738
Step Duration [s]	0.810	0.877
Step Speed [m/s]	0.859	0.842

The control method of hybrid zero dynamics (HZD)—used to design our reference gait—enables an analytical proof of orbital stability [8]. However, the virtual constraint projection does not preserve hybrid invariance, so this analytical proof is not valid for our projected gait. We will instead use the perturbation analysis procedure described in [31], [32] to numerically calculate these eigenvalues after observing convergence to a fixed point (i.e., periodic orbit).

C. Simulation Results

For comparison both the original (reference) virtual constraints and the projected virtual constraints were implemented on the prosthetic leg of the amputee biped model. Both simulations converged to (different) two-step periodic orbits. A numerical analysis found that the maximum absolute eigenvalue of the linearized Poincaré map was 0.79 about the original periodic orbit and 0.55 about the projected periodic orbit, implying both gaits are (locally) stable. Hence, the projection did not significantly alter the stability properties of the HZD-based virtual constraints.

The projection provided slight flexibility in the joint kinematics but did not significantly interfere with the prosthetic leg's ability to track the reference virtual constraints. Little tracking error can be seen in the prosthetic joint trajectories plotted over the phase variable in Fig. 2 (left). The projection also did not significantly change the magnitudes of the joint torques except immediately after impact events (Fig. 2, right). However, temporal differences are clear in the phase variable trajectory (Fig. 3) and phase portraits (Fig. 4) of the prosthetic leg. Although the prosthesis reasonably tracked the reference joint angles over the phase variable, the small deviations in Fig. 2 were sufficient to slow the phase variable and the prosthetic leg's progression through its joint patterns. In fact, the projected gait had a slower step velocity and longer step period compared to the original gait, whereas the step length was largely unchanged in Table I.

V. DISCUSSION AND CONCLUSION

Although we achieved our goal of output invariance with respect to all interaction force directions during swing, only one direction could be nullified during stance. In the presence of two contact constraints during stance, the dimension of the internal dynamics (9) reduces from 6 to 2, corresponding

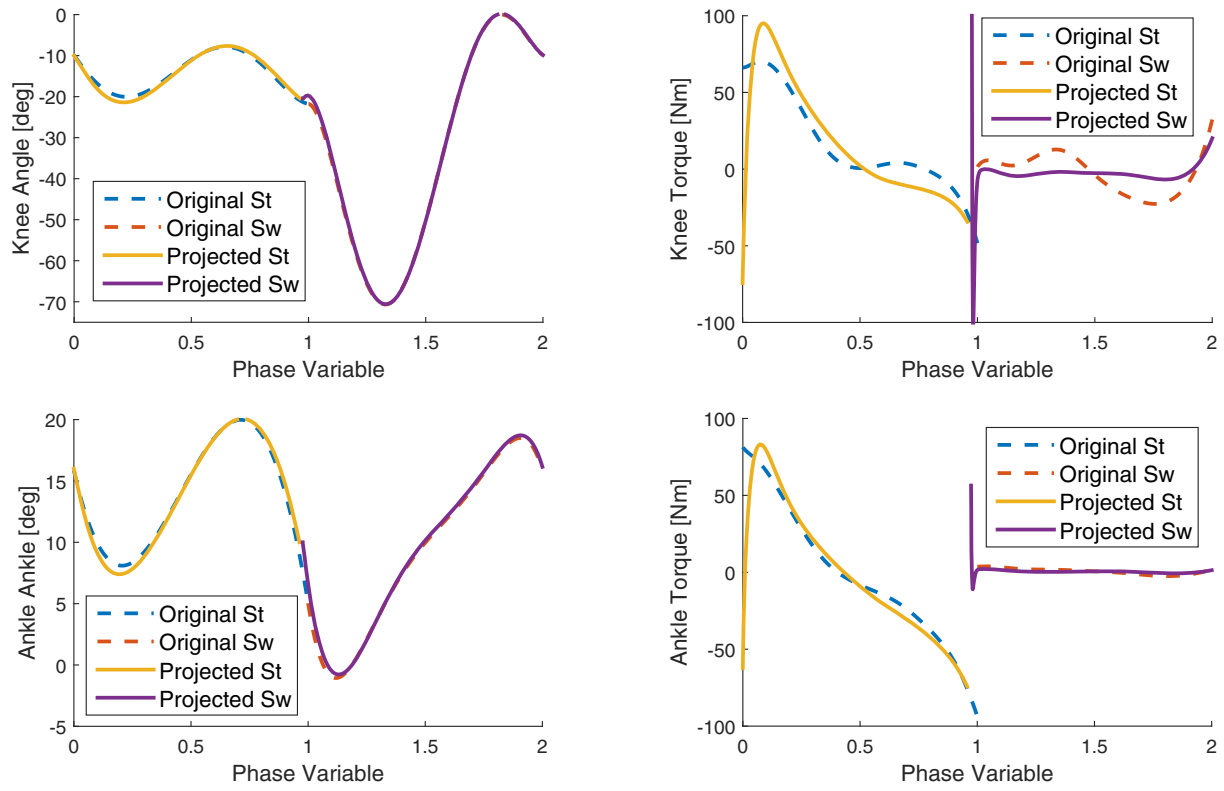

Fig. 2. Joint trajectories (left) and torques (right) over normalized phase variable for the prosthetic knee (top) and ankle (bottom) with the original virtual constraints (dashed) and the projected virtual constraints (solid). The prosthesis stance period (St) is indicated by phase values from 0 to 1, whereas the prosthesis swing period (Sw) is indicated by values from 1 to 2 for visualization purposes.

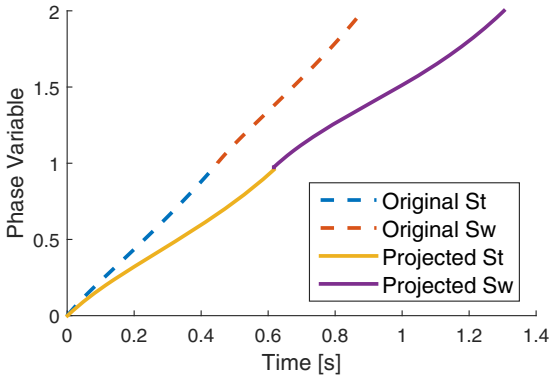

Fig. 3. Normalized phase variable (hip position) over time with the original virtual constraints (dashed) and the projected virtual constraints (solid). The prosthesis stance period (St) is indicated by phase values from 0 to 1, whereas the prosthesis swing period (Sw) is indicated by values from 1 to 2 for visualization purposes.

to the position and velocity of the unactuated DOF q_1. It is possible that only one direction of the interaction forces can be fully embedded in 2-dimensional internal dynamics, which would explain why we were only able to satisfy condition (26) for the nullspace in the F_x direction. This analytical question will be the topic of future investigation.

The observed effect of the projection on walking speed might be explained by the choice of nullspace in the F_x direction, which is approximately the direction of locomotion. In theory this could allow the human user to determine the walking speed without resistance from the prosthesis, which would no longer produce forces to exactly track the reference trajectories in opposition to the horizontal interaction force. Because the amputee model's controller was not designed to maintain a particular speed, the walking speed of the biped model decreased when the prosthesis no longer forced the original walking speed. Alternatively, it is possible that this projection could prevent propulsion by the prosthesis, which would have undesirable energetic consequences in amputee gait. More investigation is needed, but these simulations provide initial evidence that interaction nullspace projection, even in one force direction during stance, could substantially affect the cooperation between the prosthesis and its user.

This paper utilized input-output feedback linearization to enforce the projected virtual constraints, but other nonlinear output regulation techniques could also benefit from the projection (e.g., acceleration-based inverse dynamics [25], adaptive control [29], or robust control methods [5]). Future work will attempt to analytically prove the possible directions of nullspace projection during stance. Notions of hybrid invariance and hybrid zero dynamics could also be investigated with projected virtual constraints. Finally, only experiments with a prosthetic leg can determine whether or not human subjects prefer virtual constraints that have been projected into the interaction nullspace.

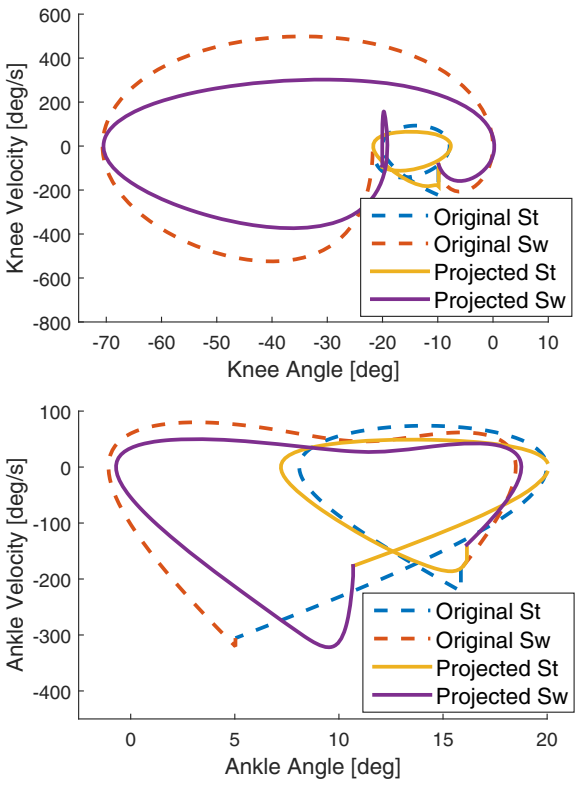

Fig. 4. Phase portraits of the prosthetic knee (top) and ankle (bottom) with the original virtual constraints (dashed) and the projected virtual constraints (solid) for the complete stride, i.e., prosthetic stance and swing.

REFERENCES

[1] F. Sup, A. Bohara, and M. Goldfarb, "Design and control of a powered transfemoral prosthesis," *Int. J. Robot. Res.*, vol. 27, no. 2, pp. 263–273, 2008.

[2] F. Sup, H. Varol, and M. Goldfarb, "Upslope walking with a powered knee and ankle prosthesis: Initial results with an amputee subject," *IEEE Trans Neural Sys Rehab Eng*, vol. 19, no. 1, pp. 71–78, 2011.

[3] M. R. Tucker, J. Olivier, A. Pagel, H. Bleuler, M. Bouri, O. Lambercy, J. del R Millán, R. Riener, H. Vallery, and R. Gassert, "Control strategies for active lower extremity prosthetics and orthotics: a review," *J. Neuroengineering and Rehabilitation*, vol. 12, no. 1, 2015.

[4] A. Nanjangud and R. D. Gregg, "Simultaneous control of an ankle-foot prosthesis model using a virtual constraint," in *ASME Dynamic Systems Control Conf.*, San Antonio, TX, 2014.

[5] K. A. Hamed and R. D. Gregg, "Decentralized feedback controllers for exponential stabilization of hybrid periodic orbits: Application to robotic walking," in *American Control Conference*, 2016.

[6] A. Isidori, *Nonlinear Control Systems: An Introduction*, 3rd ed. Berlin, Germany: Springer-Verlag, 1995.

[7] R. D. Gregg, T. Lenzi, L. J. Hargrove, and J. W. Sensinger, "Virtual constraint control of a powered prosthetic leg: From simulation to experiments with transfemoral amputees," *IEEE Trans. Robotics*, vol. 30, no. 6, pp. 1455–1471, 2014.

[8] A. E. Martin and R. D. Gregg, "Hybrid invariance and stability of a feedback linearizing controller for powered prostheses," in *American Control Conference*, 2015, pp. 4670–4676.

[9] E. Westervelt, J. Grizzle, C. Chevallereau, J. Choi, and B. Morris, *Feedback Control of Dynamic Bipedal Robot Locomotion*. New York, NY: CRC Press, 2007.

[10] E. R. Westervelt, J. W. Grizzle, and D. E. Koditschek, "Hybrid zero dynamics of planar biped walkers," *IEEE Trans. Automat. Contr.*, vol. 48, no. 1, pp. 42–56, 2003.

[11] K. Sreenath, H. W. Park, I. Poulakakis, and J. W. Grizzle, "A compliant hybrid zero dynamics controller for stable, efficient and fast bipedal walking on MABEL," *Int. J. Robot. Res.*, vol. 30, no. 9, pp. 1170–1193, 2011.

[12] I. Poulakakis and J. W. Grizzle, "The spring loaded inverted pendulum as the hybrid zero dynamics of an asymmetric hopper," *Automatic Control, IEEE Transactions on*, vol. 54, no. 8, pp. 1779–1793, 2009.

[13] S. Kolathaya and A. D. Ames, "Achieving bipedal locomotion on rough terrain through human-inspired control," in *IEEE Int. Sym. Safety Security Rescue Robot.*, College Station, TX, 2012.

[14] A. Martin, D. Post, and J. Schmiedeler, "Design and experimental implementation of a hybrid zero dynamics controller for planar bipeds with curved feet," *Int. J. Robot. Res.*, vol. 33, no. 7, pp. 988–1005, 2014.

[15] A. Ramezani, J. W. Hurst, K. A. Hamed, and J. W. Grizzle, "Performance analysis and feedback control of ATRIAS, a 3D bipedal robot," *ASME J. Dyn. Sys. Meas. Control*, vol. 136, no. 2, p. 021012, 2013.

[16] K. Akbari Hamed, B. Buss, and J. Grizzle, "Continuous-time controllers for stabilizing periodic orbits of hybrid systems: Application to an underactuated 3D bipedal robot," in *IEEE Conf. Decision & Control*, 2014, pp. 1507–1513.

[17] K. A. Hamed, B. G. Buss, and J. W. Grizzle, "Exponentially stabilizing continuous-time controllers for periodic orbits of hybrid systems: Application to bipedal locomotion with ground height variations," *Int. J. Robotics Research*, 2015, OnlineFirst.

[18] A. Martin and J. Schmiedeler, "Predicting human walking gaits with a simple planar model," *J. Biomech.*, vol. 47, no. 6, pp. 1416–1421, 2014.

[19] G. Lv and R. D. Gregg, "Orthotic body-weight support through underactuated potential energy shaping with contact constraints," in *IEEE Conf. Decision & Control*, 2015.

[20] R. M. Murray, Z. Li, and S. S. Sastry, *A Mathematical Introduction to Robotic Manipulation*. Boca Raton, FL: CRC Press, 1994.

[21] H. K. Khalil, *Nonlinear Systems*, 3rd ed. Upper Saddle River, NJ: Prentice Hall, 2002.

[22] C. D. Meyer, *Matrix Analysis and Applied Linear Algebra*. Philadelphia, PA: Siam, 2000.

[23] J. Nakanishi, R. Cory, M. Mistry, J. Peters, and S. Schaal, "Operational space control: A theoretical and empirical comparison," *Int. J. Robot. Res.*, vol. 27, no. 6, pp. 737–757, 2008.

[24] L. Sentis and O. Khatib, "Synthesis of whole-body behaviors through hierarchical control of behavioral primitives," *Int. J. Humanoid Robot.*, vol. 2, no. 4, pp. 505–518, 2005.

[25] R. D. Gregg and L. Righetti, "Controlled reduction with unactuated cyclic variables: Application to 3D bipedal walking with passive yaw rotation," *IEEE Trans. Automat. Contr.*, vol. 58, no. 10, pp. 2679–2685, 2013.

[26] D. S. Bernstein, *Matrix Mathematics: Theory, Facts, and Formulas*. Princeton University Press, 2009.

[27] R. D. Gregg, T. Lenzi, N. P. Fey, L. J. Hargrove, and J. W. Sensinger, "Experimental effective shape control of a powered transfemoral prosthesis," in *IEEE Int. Conf. Rehab. Robot.*, Seattle, WA, 2013.

[28] A. D. Ames, K. Galloway, J. W. Grizzle, and K. Sreenath, "Rapidly exponentially stabilizing control Lyapunov functions and hybrid zero dynamics," *IEEE Trans. Automat. Contr.*, vol. 59, no. 4, pp. 876–891, 2014.

[29] Q. Nguyen and K. Sreenath, "L_1 adaptive control for bipedal robots with control lyapunov function based quadratic programs," in *American Control Conference*, 2015, pp. 862–867.

[30] D. J. Villarreal and R. D. Gregg, "A survey of phase variable candidates of human locomotion," in *IEEE Int. Conf. Eng. Med. Biol. Soc.*, Chicago, IL, 2014, pp. 4017–4021.

[31] A. Goswami, B. Thuilot, and B. Espiau, "Compass-like biped robot part I: Stability and bifurcation of passive gaits," Institut National de Recherche en Informatique et en Automatique (INRIA), Grenoble, France, Tech. Rep. 2996, 1996.

[32] R. D. Gregg, Y. Y. Dhaher, A. Degani, and K. M. Lynch, "On the mechanics of functional asymmetry in bipedal walking," *IEEE Trans. Biomed. Eng.*, vol. 59, no. 5, pp. 1310–1318, 2012.